



MEaSURES BedMachine Antarctica, Version 2

USER GUIDE

How to Cite These Data

As a condition of using these data, you must include a citation:

Morlighem, M. 2020. *MEaSURES BedMachine Antarctica, Version 2*. [Indicate subset used]. Boulder, Colorado USA. NASA National Snow and Ice Data Center Distributed Active Archive Center. <https://doi.org/10.5067/E1QL9HFQ7A8M>. [Date Accessed].

We also request that you acknowledge the author(s) of this data set by referencing the following peer-reviewed publication:

Morlighem, M., E. Rignot, T. Binder, D. D. Blankenship, R. Drews, G. Eagles, O., et al. 2020. Deep glacial troughs and stabilizing ridges unveiled beneath the margins of the Antarctic ice sheet, *Nature Geoscience*. 13. 132-137. <https://doi.org/10.1038/s41561-019-0510-8>

FOR QUESTIONS ABOUT THESE DATA, CONTACT NSIDC@NSIDC.ORG

FOR CURRENT INFORMATION, VISIT <https://nsidc.org/data/NSIDC-0756>



National Snow and Ice Data Center

TABLE OF CONTENTS

1	DATA DESCRIPTION.....	2
1.1	Parameters	2
1.2	File Information	2
1.2.1	Format	2
1.2.2	File Contents	2
1.2.3	Naming Convention	4
1.3	Spatial Information	4
1.3.1	Coverage	4
1.3.2	Resolution.....	4
1.3.3	Geolocation	4
1.4	Temporal Information	5
1.4.1	Coverage	5
2	DATA ACQUISITION AND PROCESSING	5
2.1	Input Data	5
2.2	Mapping Methods.....	6
2.3	Processing Steps	7
2.4	Data Quality and Errors.....	8
3	SOFTWARE AND TOOLS.....	9
4	VERSION HISTORY	9
5	RELATED DATA SETS	10
6	RELATED WEBSITES.....	10
7	CONTACTS AND ACKNOWLEDGMENTS.....	10
8	REFERENCES	10
9	DOCUMENT INFORMATION.....	12
9.1	Publication Date	12
9.2	Date Last Updated	12

1 DATA DESCRIPTION

1.1 Parameters

This data set contains a bed topography/bathymetry map of Antarctica derived via mass conservation, streamline diffusion, and other methods.

Secondary parameters included are ice thickness and ice surface elevation. The surface elevation is taken from the Reference Elevation Model of Antarctica (REMA) and the bed is deduced by subtracting the ice thickness from the surface elevation. Also included is a firn correction parameter, which accounts for the air content of the firn layer. Ice thickness and ice surface elevation are reported in ice equivalent, meaning that the firn correction is accounted for. Table 1 includes a brief description of these parameters and their units; please refer to “Section 2.3 | Processing Steps” for details on how the parameters were derived.

Other parameters included are errors in the ice thickness/bed estimation, an ice/ocean/land mask, a source map that shows which method was employed where, and the geoid height above WGS84 ellipsoid. All parameters are heights except for the mask and the source map, which are categorical. All heights are referenced to mean sea level using the geoid EIGEN-6C4. To convert the heights to heights referenced to the WGS84 ellipsoid, simply add them to the geoid height parameter provided:

$$Z_{\text{ellipsoid}} = Z_{\text{geoid}} + \text{geoid}$$

1.2 File Information

1.2.1 Format

A single netCDF-4 file, CF-1.7 compliant.

1.2.2 File Contents

All parameters included in the data file are described in Table 1 below:

Table 1. File Parameters and Units

Parameter Name	Description	Units	Valid Range	Type
bed	bed topography (bed elevation)	meters	[-9000, 5000]	float
errbed	bed topography/ice thickness error	meters	[0, 1000]	short
firn	firn air content	meters	[0, 50]	float
geoid	geoid height difference from WGS 84 ellipsoid	meters	[-80, 80]	short
mapping	mapping attributes	-	-	char
mask	ocean/ice/land mask [0 = ocean, 1 = ice-free land, 2 = grounded ice, 3 = floating ice, 4 = Lake Vostok]	categories	[0, 4]	byte
source	data source (mapping of the methods) [1 = REMA/IBCSO, 2 = mass conservation, 3 = interpolation, 4 = hydrostatic equilibrium, 5 = streamline diffusion, 6 = gravity inversion, 7 = seismic, 10 = multibeam]	categories	[1,10]	byte
surface	ice surface elevation	meters	[0, 5000]	float
thickness	ice thickness	meters	[0, 5000]	float
x	projection x coordinate	meters	[-3333000, 3333001]	int
y	projection y coordinate	meters	[-3333000, 3333001]	int

As examples, Figure 1 illustrates how the bed topography and ice thickness maps can be displayed in Panoply:

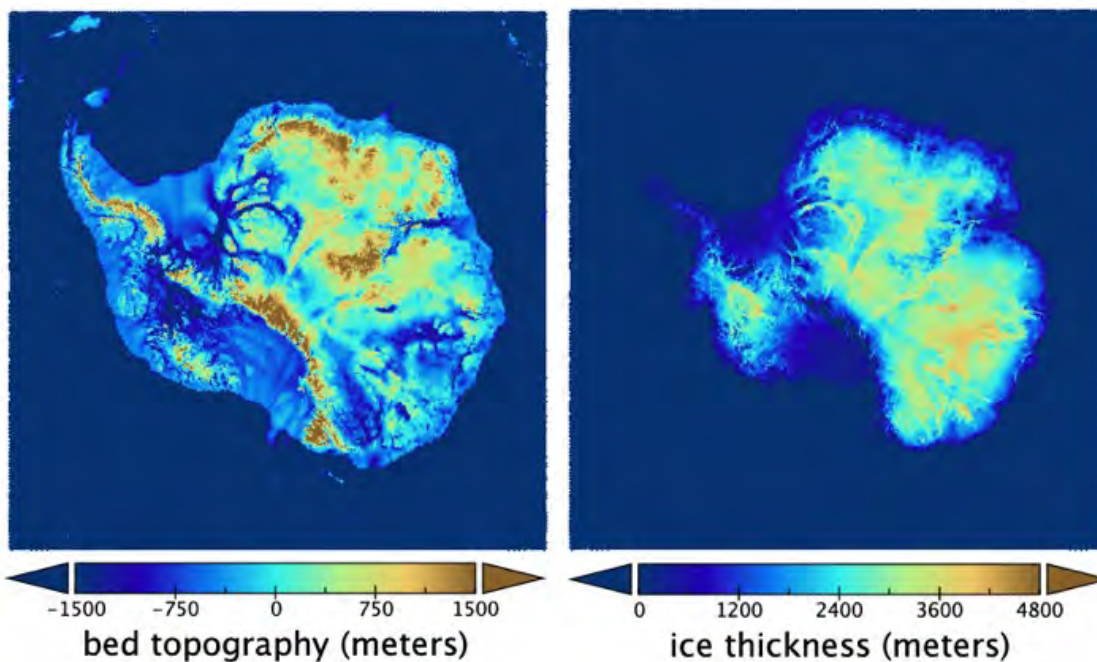


Figure 1. Maps of bed topography (left) and ice thickness (right) as displayed by Panoply version 4.10.10.

1.2.3 Naming Convention

The file name is `BedMachineAntarctica_2020-07-15_v02.nc`, where `BedMachineAntarctica` is the data set name, `2020-07-15` is the version production date, and `v02` stands for Version 2.

1.3 Spatial Information

1.3.1 Coverage

Antarctic polar region south of 70° S.

1.3.2 Resolution

500 meters

1.3.3 Geolocation

i This data set is nominally provided in EPSG:3031: the Antarctic Polar Stereographic projection based on WGS 84. However, the tool used to convert latitudes and longitudes to polar stereographic coordinates was based on the Hughes Ellipsoid. As such, the resulting inverse flattening attribute (298.2794050428205) differs slightly from the EPSG:3031, WGS 84 defined value (298.257223563).

Table 2 provides information for geolocating this data set:

Table 2. Geolocation Details

Geographic coordinate system	WGS 84
Projected coordinate system	WGS 84 / Antarctic Polar Stereographic
Longitude of true origin	0° E
Latitude of true origin	71° S
Scale factor at longitude of true origin	1
Datum	WGS 84
Ellipsoid/spheroid	WGS 84
Units	meter
False easting	0
False northing	0
EPSG code	3031
PROJ4 string	<code>+proj=stere +lat_0=-90 +lat_ts=-71 +lon_0=0 +k=1 +x_0=0 +y_0=0 +datum=WGS84 +units=m +no_defs</code>
Reference	https://epsg.io/3031

1.4 Temporal Information

1.4.1 Coverage

The data were collected between 01 January 1970 and 01 October 2019. The nominal year of this data set is 2015, following the year of the surface digital elevation model the data are based on.

2 DATA ACQUISITION AND PROCESSING

2.1 Input Data

Data inputs used in deriving this product include:

- Ice thickness data from Airborne Ice Penetrating Radar obtained during 47 survey campaigns, from 1967 to present, involving 19 institutes (Figure 2 depicts the areas covered by each campaign). In Version 2, additional ice thickness data from Young et al. (2017) and Cui et al. (2020) were included to constrain the bed topography under grounded ice.
- Ice-shelf bathymetry from the International Bathymetric Chart of the Southern Ocean (IBCSO; Arndt et al., 2013) improved in some places based on gravity-derived inversion from various survey measurements (Millan et al., 2017; Greenbaum et al., 2015; Tinto et al., 2019) and completed by seismic data where available (Rosier et al., 2018)
- Ice flow velocity derived from satellite interferometry (Rignot et al., 2011; Mouginot et al., 2017)
- Surface mass balance obtained with a regional atmospheric climate model (RACMO2; van Wessem et al., 2018), representative of the period 1961-1990
- Surface topography from the Reference Elevation Model of Antarctica (REMA; Howat et al., 2019)
- Ocean bathymetry from the International Bathymetric Chart of the Southern Ocean (IBCSO; Arndt et al., 2013).
- Version 2 also includes new multi-beam ocean bathymetry data in the Amundsen Sea embayment (Hogan et al., 2020) as well as gravity inversions for this sector (Jordan et al., 2020).

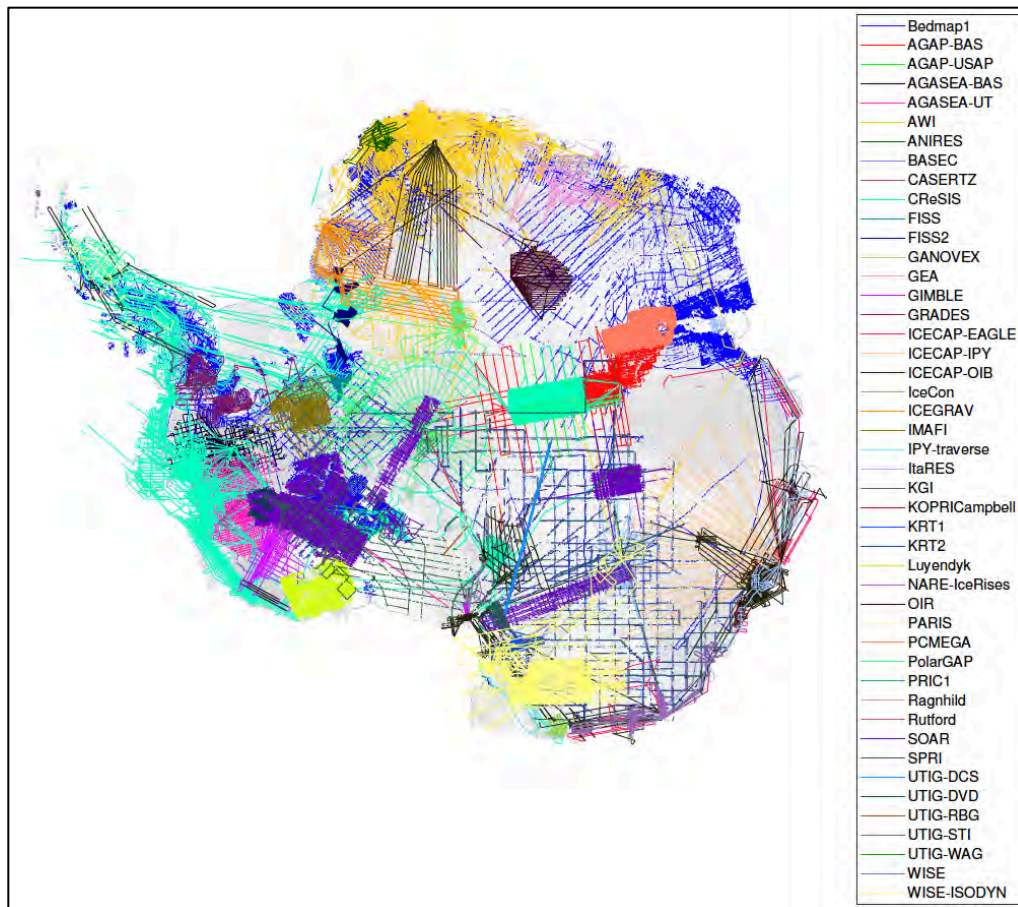


Figure 2. Airborne radar sounding tracks from which ice thickness data were derived (adapted from Figure S2 in Morlighem et al., 2020). For references and institutions involved in each campaign, please see Table S1 in Morlighem et al. (2020).

2.2 Mapping Methods

Figure 3 depicts the regions across the Antarctic continent where each mapping method was employed. Namely, mass conservation was used to map ice thickness in regions of fast-moving ice, streamline diffusion in regions of slow-moving ice, hydrostatic equilibrium for floating ice shelves, and gravity inversion and seismic bathymetry for grounded ice shelves.

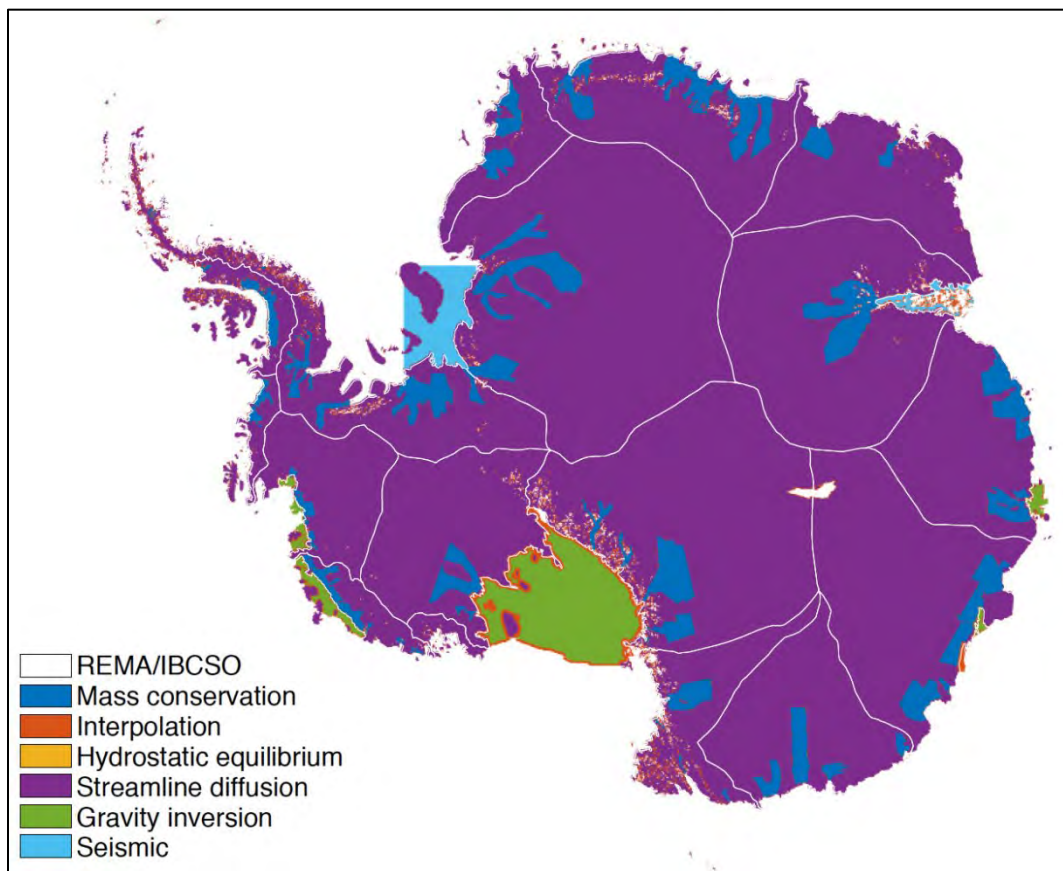


Figure 3. Mapping methods applied across the Antarctic continent (adapted from Figure S1 in Morlighem et al., 2020).

2.3 Processing Steps

The Mass Conservation (MC) method yields ice thickness and bed topography compatible with ice sheet numerical models, resolves uncertainties of prior interpretation of radar echoes, and ensures that grounding line fluxes are compatible with snowfall accumulation and thinning rates in the interior without assuming steady-state. Ice surface motion provides a physical basis for extrapolating sparse ice thickness data to larger areas with few or no data. The method works best in areas of fast flow (i.e., ice surface velocity > 30 m/yr), where errors in flow direction are small and the glaciers slide on the bed.

The MC method combines sparse, airborne, radar-sounding-derived ice thickness data with high-resolution ice motion derived from satellite interferometric synthetic-aperture radar and mass balance to estimate ice thickness across the entire continent. The algorithm conserves mass fluxes while minimizing the departure from the original radar-derived ice thickness data. The mathematical formulae of this method are summarized in Morlighem et al. (2019, Supplementary Information) and extensively detailed in Morlighem et al. (2011, 2014, 2017).

In the interior slow-moving sectors, where errors in flow direction are larger, a streamline diffusion method is used to interpolate ice thickness. This method was chosen as an alternative to more commonly used methods such as kriging or splines because it is better at capturing the intrinsic anisotropy of the ice thickness that mass conservation requires: as ice is transported downstream, ice thickness varies slowly along the flow. Across flow, significantly higher gradients in ice thickness are expected. The diffusion equation accounts for this asymmetry. While not based on physics, it is a way to interpolate ice thickness between flight lines anisotropically. See Morlighem et al. (2019, Supplementary Information) for more details.

On floating ice shelves, hydrostatic equilibrium is applied with a calibrated firn depth correction so the inferred ice thickness is consistent with available ice shelf thickness data, thus ensuring continuity in ice thickness across the grounding line.

Individual MC ice thickness maps are constrained by flight lines along their boundaries. All the MC maps are stitched together using simple interpolation (inverse distance weighting), and combined with the ice thickness maps derived via streamline diffusion. The Antarctic bed topography is derived by subtracting the resulting ice thickness map from the REMA surface digital elevation model (Howat et al., 2019). Over ice-free land areas, the bed topography is the REMA itself.

The surface elevation and ice thickness maps provided in this data set are given in ice equivalent, as they include the firn air content correction (i.e., they are lower than they would be if the air column height was included). The elevation of the top of the snow as provided by REMA can be reconstructed by adding the firn depth correction (firn air content) to the ice surface elevation provided in the data file:

$$S_{REMA} = S_{BedMachine} + d_{firn}$$

2.4 Data Quality and Errors

Sources of error include error in ice velocity direction and magnitude, error in surface mass balance, and ice thinning rates.

In a trial setting with unusually dense radar sounding coverage, errors in the MC-inferred thickness are reported at 36 m, only slightly higher than that of the original data. In areas less well constrained by radar-derived thickness data, or constrained by only one track of data, for example, in East Antarctica, errors may (well) exceed 200 m (Morlighem et al., 2020).

No or very little data were available for some ice shelf bathymetry, and uncertainty may be high (> 500 m). Version 2 includes the correction of an error in geoid height identified in the IBCSO bathymetry.

Error estimates of the bed elevation and ice thickness are provided in the data set (Figure 4).

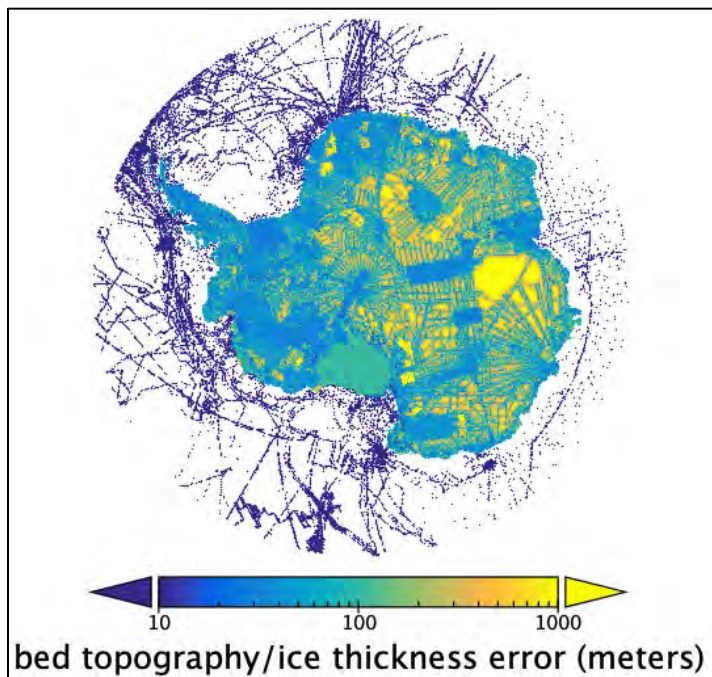


Figure 4. Spatial distribution of errors in the estimation of bed topography/ice thickness, as displayed by Panoply version 4.10.10. Note that the color bar is on a logarithmic scale.

3 SOFTWARE AND TOOLS

There are a number of netCDF file readers available to read/view netCDF files. For a list of some of these tools, please see the [NetCDF Resources at NSIDC: Software and Tools](#) Web page.

4 VERSION HISTORY

Table 3. Version History Summary

Version	Release Date	Description of Changes
V1	December 2019	Initial release
V2	September 2020	Changes to this version include: <ul style="list-style-type: none"> • additional thickness data to constrain the bed topography under grounded ice • new multi-beam bathymetry data, as well as gravity inversions, integrated in the Amundsen Sea embayment • an error in geoid height was corrected for the IBCSO bathymetry

5 RELATED DATA SETS

[IceBridge BedMachine Greenland](#)

6 RELATED WEBSITES

[NASA MEaSURES Data at NSIDC](#)

[NASA MEaSURES](#)

[Antarctic Ice Sheet Velocity \(AIV\) and Mapping Data at NSIDC](#)

7 CONTACTS AND ACKNOWLEDGMENTS

Mathieu Morlighem

University of California Irvine

8 REFERENCES

Arndt, J. E., Schenke, H. W., Jakobsson, M., Nitsche, F. O., Buys, G., Goleby, B., et al. (2013). The International Bathymetric Chart of the Southern Ocean (IBCSO) Version 1.0-A new bathymetric compilation covering circum-Antarctic waters. *Geophysical Research Letters*, 40(12), 3111–3117.

<https://doi.org/10.1002/grl.50413>

Cui, X., Jeofry, H., Greenbaum, J. S., Guo, J., Li, L., Lindzey, L. E., Habbal, F. A., Wei, W., Young, D. A., Ross, N., Morlighem, M., Jong, L. M., Roberts, J. L., Blankenship, D. D., Bo, S., & Siegert, M. J. (2020). Bed topography of Princess Elizabeth Land in East Antarctica. Copernicus GmbH.

<https://doi.org/10.5194/essd-2020-126>

Greenbaum, J. S., Blankenship, D. D., Young, D. A., Richter, T. G., Roberts, J. L., Aitken, A. R. A., et al. (2015). Ocean access to a cavity beneath Totten Glacier in East Antarctica. *Nature Geoscience*, 8(4), 294–298.

<https://doi.org/10.1038/ngeo2388>

Hogan, K. A., Larter, R. D., Graham, A. G. C., Arthern, R., Kirkham, J. D., Totten Minzoni, R., Jordan, T. A., Clark, R., Fitzgerald, V., Wåhlin, A. K., Anderson, J. B., Hillenbrand, C.-D., Nitsche, F. O., Simkins, L., Smith, J. A., Gohl, K., Arndt, J. E., Hong, J., & Wellner, J. (2020). Revealing the former bed of Thwaites Glacier using sea-floor bathymetry: implications for warm-water routing and bed controls on ice flow and buttressing. *The Cryosphere*, 14(9), 2883–2908.

<https://doi.org/10.5194/tc-14-2883-2020>

Howat, I. M., Porter, C., Smith, B. E., Noh, M.-J., & Morin, P. (2019). The Reference Elevation Model of Antarctica. *The Cryosphere*, 13(2), 665–674.

<https://doi.org/10.5194/tc-13-665-2019>

Jordan, T. A., Porter, D., Tinto, K., Millan, R., Muto, A., Hogan, K., Larter, R. D., Graham, A. G. C., & Paden, J. D. (2020). New gravity-derived bathymetry for the Thwaites, Crosson, and Dotson ice shelves revealing two ice shelf populations. *The Cryosphere*, 14(9), 2869–2882.

<https://doi.org/10.5194/tc-14-2869-2020>

Millan, R., Rignot, E., Bernier, V., Morlighem, M., & Dutrieux, P. (2017). Bathymetry of the Amundsen Sea Embayment sector of West Antarctica from Operation IceBridge gravity and other data. *Geophysical Research Letters*, 44(3), 1360–1368. <https://doi.org/10.1002/2016gl072071>

Morlighem, M., Rignot, E., Seroussi, H., Larour, E., Ben Dhia, H., & Aubry, D. (2011). A mass conservation approach for mapping glacier ice thickness. *Geophysical Research Letters*, 38(19), 1-6. <https://doi.org/10.1029/2011gl048659>

Morlighem, M., Rignot, E., Mouginot, J., Seroussi, H., & Larour, E. (2014). Deeply incised submarine glacial valleys beneath the Greenland ice sheet. *Nature Geoscience*, 7(6), 418–422.

<https://doi.org/10.1038/ngeo2167>

Morlighem, M., Williams, C. N., Rignot, E., An, L., Arndt, J. E., Bamber, J. L., et al. (2017). BedMachine v3: Complete Bed Topography and Ocean Bathymetry Mapping of Greenland From Multibeam Echo Sounding Combined With Mass Conservation. *Geophysical Research Letters*, 44(21), 11,051-11,061. <https://doi.org/10.1002/2017gl074954>

Morlighem, M., Rignot, E., Binder, T., Blankenship, D., Drews, R., Eagles, G., et al. (2020). Deep glacial troughs and stabilizing ridges unveiled beneath the margins of the Antarctic ice sheet.

Nature Geoscience, 13, 132–137. <https://doi.org/10.1038/s41561-019-0510-8>

Mouginot, J., Rignot, E., Scheuchl, B., & Millan, R. (2017). Comprehensive Annual Ice Sheet Velocity Mapping Using Landsat-8, Sentinel-1, and RADARSAT-2 Data. *Remote Sensing*, 9(4), 364. <https://doi.org/10.3390/rs9040364>

Rignot, E., Velicogna, I., van den Broeke, M. R., Monaghan, A., & Lenaerts, J. T. M. (2011). Acceleration of the contribution of the Greenland and Antarctic ice sheets to sea level rise.

Geophysical Research Letters, 38(5), n/a-n/a. <https://doi.org/10.1029/2011gl046583>

Rosier, S. H. R., Hofstede, C., Brisbourne, A. M., Hattermann, T., Nicholls, K. W., Davis, P. E. D., et al. (2018). A New Bathymetry for the Southeastern Filchner-Ronne Ice Shelf: Implications for Modern Oceanographic Processes and Glacial History. *Journal of Geophysical Research: Oceans*, 123(7), 4610–4623. <https://doi.org/10.1029/2018jc013982>

Tinto, K. J., Padman, L., Siddoway, C. S., Springer, S. R., Fricker, H. A., Das, I., et al. (2019). Ross Ice Shelf response to climate driven by the tectonic imprint on seafloor bathymetry. *Nature Geoscience*, 12(6), 441–449. <https://doi.org/10.1038/s41561-019-0370-2>

van Wessem, J. M., van de Berg, W. J., Noël, B. P. Y., van Meijgaard, E., Amory, C., Birnbaum, G., et al. (2018). Modelling the climate and surface mass balance of polar ice sheets using RACMO2 – Part 2: Antarctica (1979–2016). *The Cryosphere*, 12(4), 1479–1498. <https://doi.org/10.5194/tc-12-1479-2018>

Young, D. A., Roberts, J. L., Ritz, C., Frezzotti, M., Quartini, E., Cavitte, M. G. P., Tozer, C. R., Steinhage, D., Urbini, S., Corr, H. F. J., van Ommen, T., & Blankenship, D. D. (2017). High-resolution boundary conditions of an old ice target near Dome C, Antarctica. *The Cryosphere*, 11(4), 1897–1911. <https://doi.org/10.5194/tc-11-1897-2017>

9 DOCUMENT INFORMATION

9.1 Publication Date

September 2020

9.2 Date Last Updated

March 2022